

ORIGINAL PAPER

A Ribbon-like Structure in the Ejective Organelle of the Green Microalga *Pyramimonas parkeae* (Prasinophyceae) Consists of Core Histones and Polymers Containing N-acetyl-glucosamine



Takahiro Yamagishi^{a,1}, Akira Kurihara^b, and Hiroshi Kawai^a

^aResearch Center for Inland Seas, Kobe University, Rokkodai 1-1, Kobe 657-8501, Japan

^bFaculty of Agriculture, Kyushu University, Fukuoka 812-8581, Japan

Submitted March 26, 2015; Accepted August 20, 2015
Monitoring Editor: Linda Sperling

The green microalga, *Pyramimonas parkeae* (Prasinophyceae) has an ejective organelle containing a coiled ribbon structure resembling the ejectosome in Cryptophyta. This structure is discharged from the cell by a stimulus and extends to form a tube-like structure, but the molecular components of the structure have not been identified. Tricine-SDS-PAGE analysis indicated that the ribbon-like structure of *P. parkeae* contains some proteins and low molecular acidic polymers. Edman degradation, LC/MS/MS analyses and immunological studies demonstrated that their proteins are core histones (H3, H2A, H2B and H4). In addition, monosaccharide composition analysis of the ribbon-like structures and degradation by lysozyme strongly indicated that the ribbon-like structure consist of β (1-4) linked polymers containing N-acetyl-glucosamine. Purified polymers and recombinant histones formed glob-like or filamentous structures. Therefore we conclude that the ribbon-like structure of *P. parkeae* mainly consists of a complex of core histones (H3, H2A, H2B and H4) and polymers containing N-acetyl-glucosamine, and suggest to name the ejective organelle in *P. parkeae* the “histosome” to distinguish it from the ejectosome in Cryptophyta.

© 2015 Elsevier GmbH. All rights reserved.

Key words: Core histone; ejectosome; N-acetyl-glucosamine; *Pyramimonas parkeae*.

Introduction

Ejectisomes are the extrusive organelles containing a coiled ribbon, commonly found in the Cryptophyta. When the cells are stimulated by a physical or chemical signal the coiled ribbons become discharged from the cell, and they rapidly extend to

form a straight or slightly curved hollow tube, by the lateral inward rolling of the edges of the ribbons (Kugrens et al. 1994). It has been proposed that ejectisomes have a defensive role against predators, or assist in capturing prey (Cavalier-Smith 1982).

Caedibacter, a bacterial endosymbiont of paramecia (formerly referred to as kappa particles), contains a coiled ribbon-like structure termed R-body (Fusté et al. 1986; Lالucacat et al. 1979;

¹Corresponding author; fax +81 78 803 6698
e-mail [yamataka312@gmail.com](mailto:yamatataka312@gmail.com) (T. Yamagishi).

Quackenbush 1978, 1987; Wells and Horne 1983) that resembles the ejectisome of the cryptomonads (Anderson et al. 1964; Hausmann 1978; Hovasse 1965). R-body structures are found in some gram-negative bacterial species including the genus *Caedibacter*, and they extend in telescopic fashion by unrolling from the outside or the inside under certain conditions (Pond et al. 1989). As to the molecular components of the R-body, a series of experiments about R-body synthesis and assembly in *C. taeniospiralis* and sequencing of a plasmid pKAP298 coding the R-body demonstrated that the genes *rebA*, *rebB*, *rebC*, and/or *rebD* are involved in R-body synthesis and assembly, and *rebB* may be the major constituent of R-bodies (Heruth et al. 1994; Jeblick and Kusch 2005).

In order to clarify the evolutionary relationships among ejectisomes and R-bodies, in a previous study we isolated the discharged ribbon-like structure from the red cryptomonad, *Pyrenomonas helgolandii*, and determined sequences of four putative ejectisome ribbon-related genes, *Tri1*, *Tri2*, *Tri3-1* and *Tri3-2* (Yamagishi et al. 2012). *Tri1* was homologous to the first half of the R-body protein *rebB*, which is classified in the *rebB* superfamily domain (Yamagishi et al. 2012). *Tri2*, *Tri3-1* and *Tri3-2* were grouped in the same family of low molecular weight proteins based on statistically significant similarity to one another, and they were homologous to the latter half of *rebB* (Yamagishi et al. 2012).

Similarly the katablepharids, colorless heterotrophic flagellates that are a sister group of Cryptophyta (Okamoto and Inouye 2005), possess ejectisome-like structures, and the way they form the tubes of ribbons has been shown to be similar to that in Cryptophyta (Kugrens et al. 1994). Recently, Yabuki et al. (2014) isolated *Tri* genes from the katablepharids and this indicates that the ejectisome-like structure consists of *Tri* family proteins as in cryptomonads.

The genus *Pyramimonas* (Prasinophyceae, Chlorophyta), which belongs to the green plant lineage and is phylogenetically rather distant from Cryptophyta, also possesses an ejectisome-like structure that morphologically resembles those of cryptomonads and katablepharids (Morrall and Greenwood 1980) (Supplementary Material Fig. S1A). However, it has been reported that the discharged ribbon forms a tube by a spiral rolling of the ribbon that is a very different from the way in the cryptomonads and the katablepharids (Kugrens et al. 1994) (Supplementary Material Fig. S1A, B). Recently, it has been reported that the ribbon-like structure of *Pyramimonas gondii* was dominated

by proteins with relative molecular weights of approximately 12.5-19 kDa and two additional proteins of 23 and 26 kDa (Ammerman et al. 2014; Rhiel et al. 2013). However, the ejectisome-related components of *Pyramimonas* have not yet been identified. In this study, we aimed to identify major components of the ribbon-like structure in *Pyramimonas parkeae*, and here provide new knowledge on the ejectisome-like structure of *Pyramimonas*.

Results

Histochemical Analyses

Under fluorescence microscopy the fluorescent dye 4',6-diamidino-2-phenylindole (DAPI) strongly stained not only the nucleus but also ejectisome-like structures (Fig. 1A). Discharged ejectisome-like structures rapidly extend to form a straight or slightly curved hollow tube, and they also were strongly stained by DAPI (Fig. 1B; Supplementary Material Fig. S1). However, under UV light, the DAPI fluorescence of the ribbons before and after the release from the cell photobleached more rapidly than the fluorescence in the nucleus (data not shown). Toluidine blue, which binds to acidic substances and negatively-charged polymers, also stained the ejectisome-like structures (Fig. 1C). In contrast, a nucleic acid-specific fluorescent dye SYBR Green I did not stain ribbons before and after discharge (Fig. 1D).

Molecular Characterization

The ejectisome-like structures (ribbon-like structures) were easily discharged from the cells by the acidic stimulation method without significant damage to the cell (see Methods), and the purified ribbon-like structures were nearly free of other cellular materials (Fig. 2A-D).

By toluidine blue staining after electrophoretic separation of the ribbon-like structure by tricine-SDS-PAGE, some bands were clearly detected in the small molecular weight of 1.7 kDa and 4.6 kDa. These bands were also stained by Alcian blue, but were not stained by Coomassie brilliant blue R-250 (CBB R-250) or silver staining (data not shown), indicating they may consist of acidic polymers (Fig. 2E). A standard staining method by CBB R-250 detected four major bands of 14 kDa, 15 kDa, 16.5 kDa and 17.5 kDa (Fig. 2E). The existence of proteins in the ribbon-like structure was demonstrated by amino acid composition analysis (approximately 15% of total volume) (Supplementary Material Fig. S2).

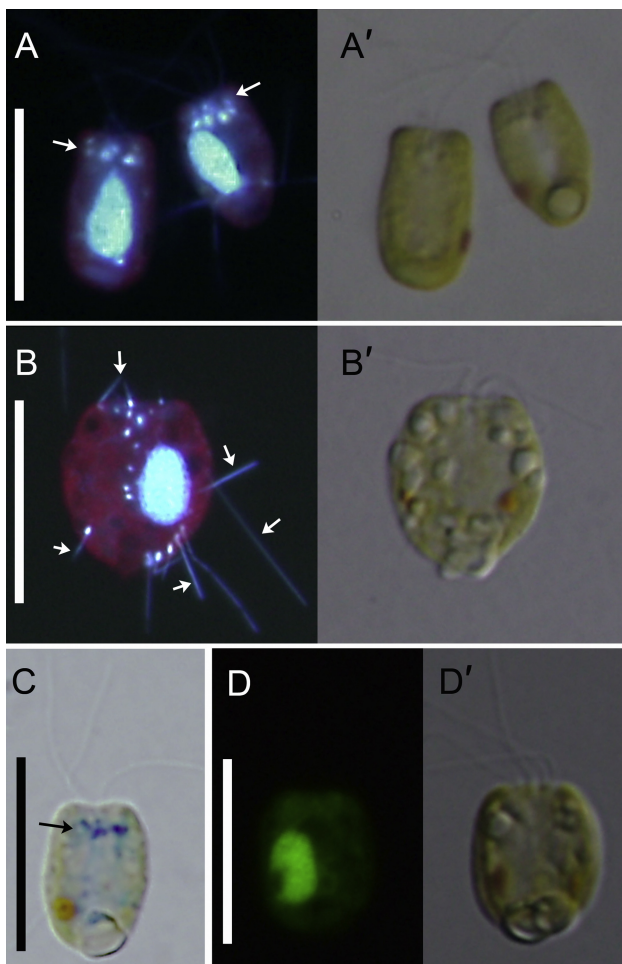


Figure 1. Fluorescence microscopy analyses of *Pyramimoas parkeae*. Cells stained with DAPI (**A** and **B**), toluidine blue (**C**), SYBR Green I (**D**) and their DIC images (**A'**). Arrows in (**A**) and (**C**) indicate ribbons before and after the release from the cell and stained by DAPI, respectively. Red and blue fluorescence in (**A**) and (**B**) show autofluorescence from the chlorophyll and DAPI fluorescence under UV, respectively. Arrow in (**C**) indicates un-discharged ribbons that were stained by toluidine blue. Scale bars, 20 μm . See also Supplementary Material Figure S1 for schematic diagrams of ejectisome-like structure.

Monosaccharide composition analysis showed that the ribbon-like structure contains five species of monosaccharide (galactose, mannose, glucose, arabinose and xylose) and one amino sugar (N-acetyl-glucosamine) (**Fig. 3**).

Edman degradation of the 17.5 kDa band detected by Coomassie staining determined 13 amino acid residues (“ARTKQTARKSTGG”) and identified it as histone H3 (**Fig. 2E**). The

proteins in 15, 14 and 16.5 kDa bands could not be determined due to blocking of the N-terminal end. Edman degradation after an in-gel digestion of the 14 kDa band using *Staphylococcus* V8 protease determined 4 amino acid residues (“HARR”) and identified it as histone H4 (**Fig. 2E**). Liquid chromatography-tandem mass spectrometry (LC/MS/MS) analyses after in-gel digestion of the 15 and 16.5 kDa bands using trypsin determined two peptide fragments (AGLQFPVGR and VGAGAPVYMAALEYLCAEVLELAGNASR) from the band of 15 kDa and two peptide fragments (QVHPDTGISSKAMSIMNSFINDLFEK and YNKKPTITSREIQTAVRLVLPGLAK) from the band of 16.5 kDa, and identified them as histones H2B and H2A, respectively (**Fig. 2E**). Western blot analyses using anti-core histone antibodies also showed that the bands of 17.5, 16.5, 15 and 14 kDa are from core histone H3, H2B, H2A and H4, respectively (**Fig. 4A**). In Edman degradation analyses of two bands (1.7 kDa and 4.6 kDa) visualized with toluidine blue and Alcian blue, no amino acids were detected. Indirect immunofluorescence microscopy using polyclonal antibodies against histone H3, H2B, H2A and H4 showed that core histones clearly localized at the ribbons before and after discharge from the cell (**Fig. 4B** and **C**). On the other hand, the nucleus was not detected by indirect immunofluorescence staining with anti-core histone antibodies (Supplementary Material **Fig. S3**).

The purified ribbon-like structures were clearly digested by proteinase K or lysozyme (**Fig. 5A,B**; Supplementary Material **Fig. S4**). Proteinase K digested most of the structure within six hours (**Fig. 5A**; Supplementary Material **Fig. S4**). Lysozyme also digested most of its structure, but not all within 24 hours (**Fig. 5B** and Supplementary Material **Fig. S4**). In electrophoretic analyses of the degraded products, toluidine blue staining showed that the small molecular weight bands of 1.7 kDa and 4.6 kDa were not digested by the proteinase K treatment, but lysozyme treatment changed these bands to smears, indicating that the contents in these bands were digested (**Fig. 5C**). CBB R-250 staining showed that proteinase K digested the core histones, but lysozyme did not affect them (**Fig. 5C**). On the other hand, DNase and RNase did not digest the ribbon-like structures, indicating that the ribbon-like structure does not contain nucleic acids (Supplementary Material **Fig. S4**).

When aliquots from the toluidine blue stained-bands (1.7 kDa and 4.6 kDa) were mixed with recombinant octamers of core histones (histone H3, H2A, H2B and H4) in vitro, globular structures rapidly appeared, and they were stained by

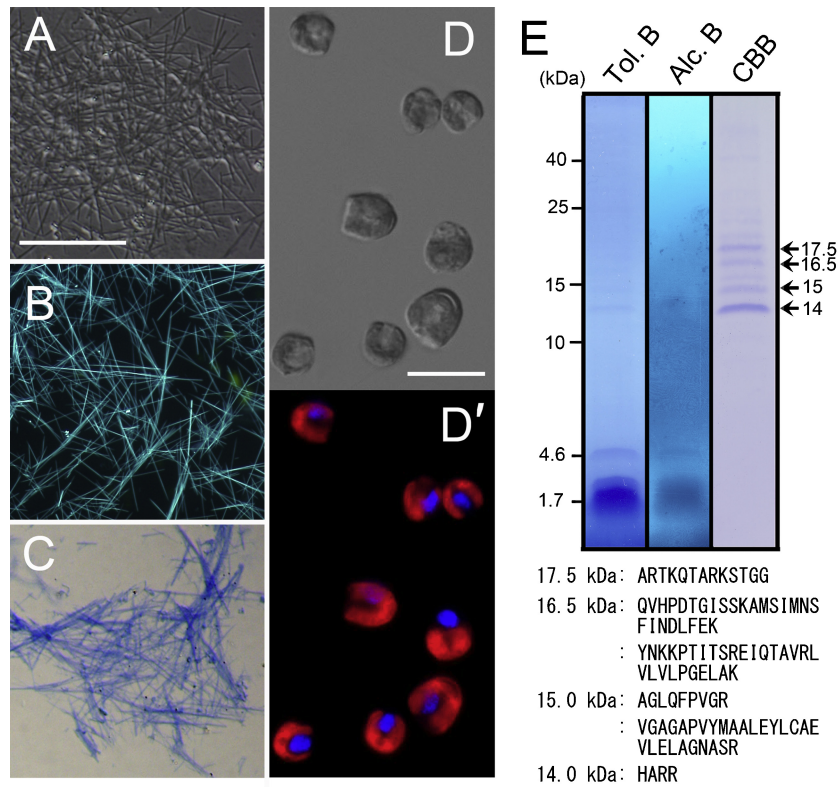


Figure 2. Images of purified ribbon-like structures of *Pyramimonas parkeae* and their tricaine-SDS-PAGE analysis. Ribbon-like structures observed by DIC (A), DAPI staining (B) and toluidine blue staining (C). DIC (D) and DAPI staining image (D') of the cells after discharging the ribbon-like structures. Red and blue colors in (D') are autofluorescence from the chlorophyll under green light and DAPI fluorescence from the nuclear under UV, respectively. Scale bar, 20 μ m. Gel images visualized by toluidine blue staining (Tol. B), Alcian blue staining (Alc. B) and standard staining with Coomassie brilliant blue R-250 (CBB) (E). Numbers in the left and right side of the gel images indicate the relative molecular weight (kDa). Fragment sequences of 17.5, 16.5, 15 and 14 kDa proteins obtained by amino acid sequencing and LC/MS/MS analyses were shown below the gel image.

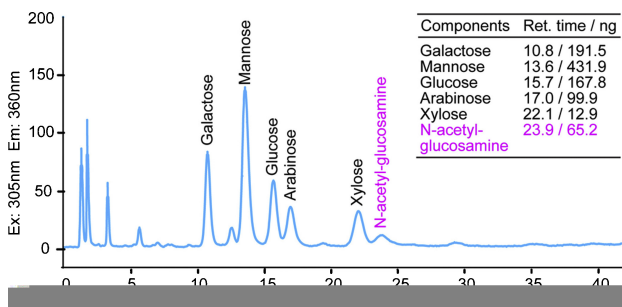


Figure 3. Monosaccharide composition analysis of the ribbon-like structures. The table indicates the retention time (min) and total quantity (ng) of found components. See also Supplementary Material Figure S2 for amino acids composition analysis of the ribbon-like structures.

indirect immunofluorescence with an anti-histone antibody and DAPI, indicating that the contents in the aliquots were associated with core histones (Fig. 5D). Filamentous structures were also found in one portion, but ribbon-like structures were not reconstructed (Fig. 5D). The aliquots never formed globular or filament-like structures by themselves.

Phylogenetic Analysis of Core Histone Proteins

Illumina HiSeq 2000 sequencing of a library from total RNA of *P. parkeae* produced 129,521 contigs (Supplementary Material Table S1). This library contained one well-identified histone H3 (*P. parkeae* H3-1), two variants of histone H2A (*P. parkeae* H2A-1 and H2A-2), one of histone H2B (*P. parkeae* H2B-1) and one of histone H4 (*P. parkeae* H4-1) (Fig. 6A; Supplementary Material



Figure 4. Western blot and immunofluorescence assay using anti-core histone antibodies. Western blot assay using anti-core histone (histone H3, H2A, H2B and H4) antibodies (**A**). Lane labeled with CBB indicates an image stained by Coomassie brilliant blue-R250 after tricine-SDS-PAGE. Numbers on the left side of the gel images indicate the relative molecular weight (kDa). Immunofluorescence microscopy analysis of ribbons after the discharge using anti-core histone (histone H3, H2A, H2B and H4) antibodies (**B**) and before the discharge from the cell using anti-histone H3 (**C**), respectively. Non-immunized rabbit serum was used as negative control. Scale bars in (A), (B) and (C), 20 μm . See also Supplementary Material Figure S3 for immunofluorescence assay during the cell cycle.

Fig. S5). Of these, *P. parkeae* H3-1, H2A-2, H2B-1 and H4-1 were consistent with the sequences of histones in the ribbon-like structure obtained by Edman degradation and LC/MS/MS analyses. In addition to these core histones, derived histone H3 (*P. parkeae* H3-derived-1) and derived histone H2A (*P. parkeae* H2A-derived-1) sequences are found in the library (Fig. 6A). Divergences of these derived histone sequences are substantially greater than that seen across broad eukaryotes (Fig. 6A; Supplementary Material Fig. S5). A library from total RNA of *Pyramimonas amyliifera* that is a species closely related to *P. parkeae*, but does not have the ejectosome-like structure, produced

119,212 contigs (Supplementary Material Table S1). Unlike the library of *P. parkeae*, this library contained only one of core histone sequences (*P. amyliifera* H2B-1) (Fig. 6A). In addition to the histone H2B sequence, three derived histone H3 (*P. amyliifera* H3-derived-1, 2 and 3) and one derived histone H2A (*P. amyliifera* H2A-derived-1) sequences were found in this library, and they also were exceptionally divergent compared to typical core histone sequences (Fig. 6A; Supplementary Material Fig. S5). Phylogenetic analyses showed that the histones in the ribbon-like structure are close to those in the plant and green algal lineage (Fig. 6B-D; Supplementary Material Fig. S6).

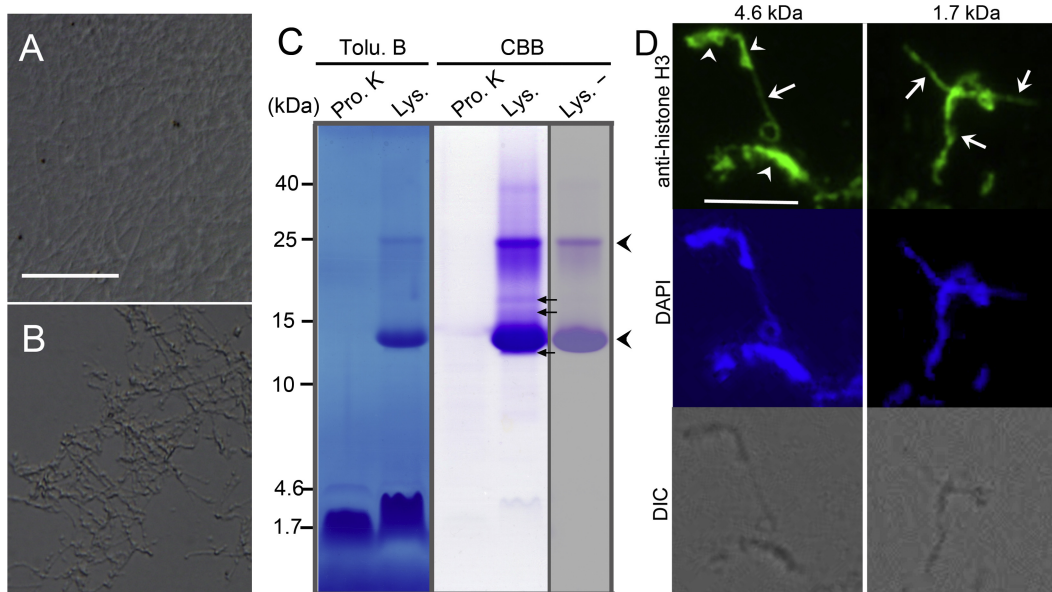


Figure 5. Enzyme digestion assays of ribbon-like structures and reconstruction assay in vitro using recombinant octamer of core histones. DIC images of purified ribbon-like structures after 6 hours of Proteinase K treatment (**A**) and after 24 hours of lysozyme treatment (**B**). See also Supplementary Material Figure S4 for proteinase K and lysozyme-treated the ribbon-like structures in detail. Proteinase K and lysozyme-treated products of the ribbon-like structures were applied to tricine-SDS-PAGE, and visualized by toluidine blue (**C**; Tolu. B). The same gel was visualized by Coomassie brilliant blue R-250 (**C**; CBB). Pro. K and Lys. indicate proteinase K and lysozyme, respectively. Lys.- indicates the control lane that only lysozyme was loaded without the substrate. Arrowheads indicate bands originated from lysozyme. Arrows indicate the band of histone H3, H2A and H4 from the top. The bands of histone H2B were overlapped with a band from lysozyme. A band of proteinase K was not detected probably because of auto-digestion by oneself. Immunofluorescence, DAPI and DIC images of assembled globs and filament-like structure in vitro (**D**). Arrowheads and arrow indicate assembled globs and filament-like structure, respectively. Scale bar, 10 μm .

Discussion

The results of immunological studies, enzymatic studies and a reconstruction assay using recombinant octamers of core histones (H3, H2A, H2B and H4) showed that the ribbon-like structure in the ejective organelle of the green alga *Pyramimonas parkeae* mainly consists of the core histones and polymers containing N-acetyl-glucosamine. It is well known that core histones associate with DNA in the nucleus, but this is the first report to show that the core histones exist apart from a nucleus.

The Ribbon-like Structure of *Pyramimonas parkeae* Contains Core Histones

Tricine-SDS-PAGE analysis of the ribbon-like structures revealed that they contain proteins with relative molecular weights of 14, 15, 16.5 and 17.5 kDa. This result substantially agrees with the report of Rhiel et al., who studied the ribbon-like structure

of *Pyramimonas grossii* by SDS-PAGE (Rhiel et al. 2013). We identified the proteins of 17.5 kDa, 16.5 kDa, 15 kDa and 14 kDa proteins histones H3, H2B, H2A and H4, respectively, based on the results of Edman degradation, LC/MS/MS and western blotting. Indirect immunofluorescence microscopy analysis using anti-core histone (histones H3, H2A, H2B and H4) antibodies demonstrated that the core histones are localized in the ribbon-like structure before and after discharge. The results of amino acid composition analysis showed that the content of lysine and arginine is high (approximately 17%), with hardly any cysteine residues, which is a distinctive feature of core histones (Supplementary Material Fig. S2). On the assumption that each of four histones (H3, H2A, H2B, and H4) would be contained in the ribbon-like structure in stoichiometric ratios, some deviations were found between the values in the amino acid composition analysis and expected values, though the most of measured amino acids were similar to the expected values (Supplementary Material Fig. S2).

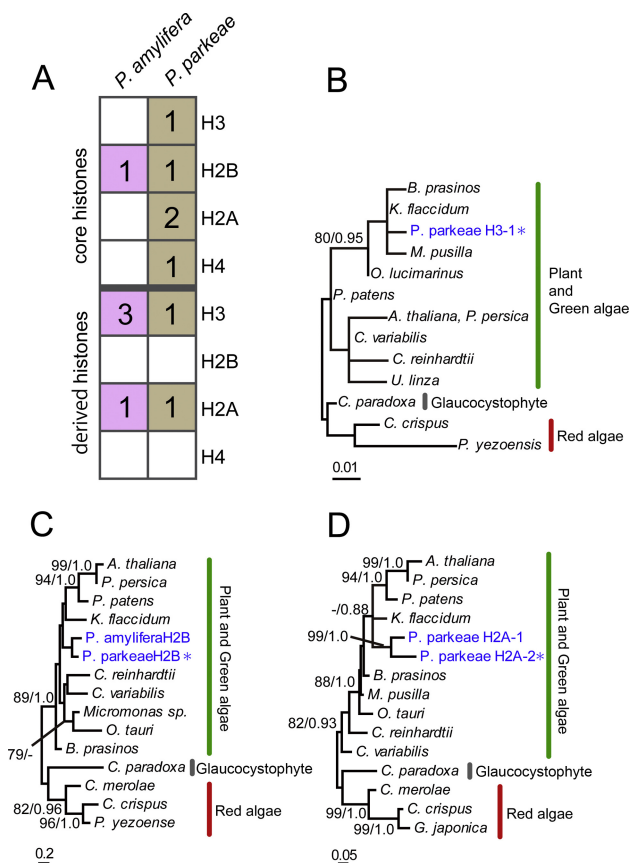


Figure 6. The relative proportion of core histone and derived histone sequences found in the library of *Pyramimonas parkeae* and *Pyramimonas amyliifera*, and the phylogenetic positions of the core histone H2A, H2B, and H3 identified from *P. parkeae* and *P. amyliifera*, inferred from the maximum-likelihood (ML) and Bayesian Inference methods. The relative proportion of core histone and histone-like sequences (**A**). Numbers in boxes indicate total number of core histone and derived histone sequences found in the library of *P. parkeae* and *P. amyliifera*. The phylogenetic trees of histone H3 (**B**), histone H2B (**C**) and histone H2A (**D**). As the two methods constructed quite similar topology, only the ML tree was shown. Left and right values at nodes represent ML bootstrap values (MLBs) and Bayesian posterior probabilities (BPPs). Only values of MLBs >70% and BPP >0.90 are shown. The sequences found in the ejectisome-like structure of *P. parkeae* were labeled with asterisk. The unit of branch length is the number of substitutions per site. See Supplementary Material Figure S5 and Table S2 for protein alignments and databases of the sequences used for the phylogenetic inferences, respectively.

Since other proteins except for the histones were not detected in the SDS-PAGE analysis, these deviations suggest that each of four histones may be contained in the ribbon-like structure in different ratios. This hypothesis is supported by the result of the SDS-PAGE analysis, in which two histones (H3 and H4) were detected in larger quantities compared to histones H2A and H2B. On the other hand, the low value of arginine may be due to the carbohydrates contained in the ribbon-like structure because sugars such as arabinose and xylose promote the destruction of arginine during acidic hydrolysis. Therefore, we conclude that most of the proteins in the ribbon-like structures consist of core histone proteins, and that they are important components in the ribbon-like structure based on the fact that the ribbon-like structures were digested by protease.

The Ribbon-like Structure of *Pyramimonas parkeae* Contains β (1-4) linked Polymers Containing N-acetylglucosamine

As toluidine blue and Alcian blue are basic dyes, they stain negatively charged and acidic polymers such as heparan sulfate, hyaluronic acid and chondroitin sulfate as well as nuclear material (Koop 1976; Scott and Dorling 1965; Volpi and Maccari 2002). The positive-staining results with toluidine blue and alcian blue in the ribbon-like structures indicate that they contain acidic or negatively charged polymers, except for core histone proteins. DAPI is a positively charged fluorescence dye with a divalent positive charge (Eriksson et al. 1993), and known to bind not only nucleic acids but also negatively charged polyphosphate (polyP), though its emission wavelength shifts from 456 nm (blue) to 540 nm (greenish-yellow) when bound to polyP (Melasniemi and Hernesmaa 2000; Tijssen et al. 1982). DAPI also binds other acidic or negatively charged polymers such as glycosaminoglycans and polyglutamic acid, with an emission wavelength similar to that of nucleic acids (Tijssen et al. 1982). The blue DAPI fluorescence in the ribbon-like structures indicates that they contain acidic or negative charged polymers other than polyP. On the other hand, the stabilities for DNase and RNase and the negative-staining result with SYBR Green I indicate that the ribbon-like structure does not contain nucleic acids. However, there is still a possibility of containing small amount of nucleic acids.

Monosaccharide composition analysis demonstrated that the ribbon-like structures contain N-acetylglucosamine. This suggests to us that

the ribbon-like structures may consist of a β (1-4) linked polymer containing N-acetyl-glucosamine as in peptidoglycan that is a main structure of cell walls in bacteria or in chitin. This hypothesis was supported by the result that lysozyme from hen white egg digested the ribbon-like structures. Lysozyme from hen white egg hydrolyzes β (1-4) linkages not only between the N-acetyl-glucosamine and N-acetylmuramic acid residues in peptidoglycan but also between the N-acetyl-glucosamine residues in chitin, therefore, in the former case the ribbon-like structure might contain N-acetylmuramic acid as a counterpart of N-acetyl-glucosamine. Monosaccharide composition analysis could not demonstrate the presence of N-acetylmuramic acid, but further optimization of acidic hydrolysis may enable the detection of N-acetylmuramic acid in the ribbon-like structure. Therefore, the linkage partner of N-acetyl-glucosamine in the ribbon-like structure is still unknown.

We also concluded that the bands of 1.7 kDa and 4.6 kDa in SDS-PAGE are components of the ribbon-like structures because they were stained by toluidine blue and Alcian blue as well as in the ribbon-like structures. Simultaneously, the contents of the bands of 1.7 kDa and 4.6 kDa are the β (1-4) linked polymers containing the N-acetyl-glucosamine based on the result that these bands were digested by lysozyme. We also consider that the polymers may consist of polysaccharides because monosaccharide composition analysis showed that the ribbon-like structures contain five monosaccharide in addition to N-acetyl-glucosamine, and these may be negatively charged with sulfate or phosphate groups. However, apart from the staining properties, there is no direct evidence for the presence of a polysaccharide in the β (1-4) linked polymers containing N-acetyl-glucosamine, and they are negatively charged. For this, it would be necessary to determine its molecular structure using NMR in the future. On the other hand, although DAPI did not stain any bands in SDS-PAGE, we think that this results from a decrease of negative electric charge by depolymerization of the ribbon-like structures.

Based on these results, we conclude that the ribbon-like structures of *P. parkeae* mainly consist of histones and the β (1-4) linked polymers containing N-acetyl-glucosamine with relative molecular weight of 1.7 kDa and 4.6 kDa, but the determination of the structure of the polymers remains to be done. This conclusion is also strongly supported by the result that the octamers of the recombinant histones and aliquots from 1.7 kDa and 4.6 kDa bands

can associate in vitro with each other, and assemble partially into globules or filament-like structures.

Origin of the Ribbon-like Structure in *Pyramimonas parkeae*

It has been reported that the ribbon-like structure of ejectisomes in cryptomonads is constituted of Tri family proteins, which have a close evolutionary relationship to the RebB protein constituting the coiled ribbon-like structure (R-body) in the bacterial endosymbiont of paramecia, *Caedibacter* (Yamagishi et al. 2012). Our present studies show that molecular components of the ribbon-like structure in *P. parkeae* differ entirely from those of cryptomonads, and have a different evolutionary origin from that of cryptomonads, indicating that ancestors of cryptomonads and *Pyramimonas* independently acquired the ejective organelle. In order to distinguish the ejectisome-like structure of *Pyramimonas* from the ejectisome of cryptomonads, we suggest to name it the “historosome”.

Recently, evidence of phagocytosis was shown in the prasinophyte *Cymbomonas*, closely related to *Pyramimonas* (Maruyama and Kim 2013). This result strongly supports a hypothesis that ejective organelles in an anterior invagination are an aid to prey capture by primitive phagotrophic flagellates (Cavalier-Smith 1982). Parke and Adams (1965) suggested that the ejective organelles remain as a relic organelle in *Pyramimonas*. However, since this assumption does not have support by a phylogenetic analysis of *Pyramimonas* species possessing and lacking ejective organelles, it is not clear whether *Pyramimonas* may have acquired the ejective organelle at a later stage or lost it during further development of autotrophic nutrition.

On the other hand, the origin of the ribbon-like structure in *P. parkeae* is very interesting, considering that the ribbon-like structure contains the core histones. Histone sequences have been identified in many archaeal genomes, and it has been suggested that eukaryotic core histones share ancestry with them, because of the histone fold (HF) structure and amino acid residues for histone-DNA and histone dimer-dimer interactions are highly conserved (Sandman and Reeve 2006). However, it remains unclear whether the ancestral proteins of the histones originated in archaea or eukaryotes, because HF-containing proteins are absent in most Crenarchaeae except for *Cenarchaeum*. Five sequences of core histones found in the library of *P. parkeae* (*P. parkeae* H3-1, H2B-1 and H2A-1, 2 and H4-1) possessed conserved HF structure and conserved amino acid

residues for histone-DNA and histone dimer-dimer interactions, and showed very close relationship to those of eukaryotes. Four of five core histone sequences (*P. parkeae* H3-1, H2B-1 and H2A-2 and H4-1) corresponded with the sequences obtained by amino acid sequencing and LC/MS/MS analyses of histones in the ribbon-like structure. This result simultaneously poses a question whether these histones in the ribbon-like structure also play a role as DNA packaging proteins in the nucleosome of *P. parkeae*. Considering the results that immunofluorescence staining using anti-core histone antibodies did not detect the nucleus of *P. parkeae* and *P. amyliifera* (data not shown), core histones may be absent from the nucleus of *P. parkeae* and *P. amyliifera* or present in very low concentration. The result that transcripts of histone H3, H2A and H4 were not found in the database of *P. amyliifera* may reflect the absence of the ejectosome in *P. amyliifera*, but it is unclear whether this is due to low expression or lack of the genes. Among eukaryotic organisms absence of core histones in the nucleus is known only in the phylum Dinoflagellata (Gornik et al. 2012). Although absence of core histones in dinoflagellates is thought to be a special case and a derived state, we consider that our present results broaden the knowledge of the evolution and origin of eukaryotic core histones. On the other hand, since some derived histone sequences were found in the library of *P. parkeae* and *P. amyliifera*, though their variations were greater than those seen across broad eukaryotic diversity, the possibility that they may act as DNA packaging proteins cannot be excluded. Also, although there is little possible technical issue with immunofluorescence staining because the method used in this study was available for detection of the nuclear histones in other some unicellular algae, SDS-PAGE analysis of nuclear-extracted proteins would be needed to elucidate whether core histones are truly absent from the nucleus of *P. parkeae* and *P. amyliifera*.

Methods

Culture: Axenic cultures of *Pyramimonas parkeae* (NIES-254) and *Pyramimonas aff. amyliifera* (NIES-251) were acquired from the Microalgal Culture Collection in the National Institute of Environmental Studies (NIES), and were cultured in EMS medium (Kasai et al. 2009) at 20 °C illuminated by white fluorescent lighting (approximately 40 $\mu\text{mol photons m}^{-2} \cdot \text{s}^{-1}$) with a 12:12 light:dark (L:D) photoperiod under gentle agitation.

Fluorescence microscopy analysis of *Pyramimonas parkeae*: Cells of *P. parkeae* were fixed for 15 min at room temperature with 3% formaldehyde (Wako Pure Chemical, Osaka, Japan) in fixation buffer (480 mM NaCl, 41.5 mM MgSO₄, 8 mM KCl, 8.25 mM Tris, and 5 mM EGTA, pH 8.0), and then adhered to a poly-L-lysine (Sigma-Aldrich, St. Louis, MO, USA) coated

coverslips. After three 1 min rinses with PBS (137 mM NaCl, 8.10 mM NaHPO₄, 2.68 mM KCl, 1.47 mM KH₂PO₄, pH 7.4), samples were stained with DAPI (1 $\mu\text{g} \cdot \text{mL}^{-1}$ in PBS), SYBR Green I (Wako Pure Chemical) or toluidine blue (Wako Pure Chemical) for 15 min at room temperature. After three 5 min rinses with PBS, samples were mounted in 50% glycerol-PBS containing 0.1% *p*-phenylenediamine and observed with a BX-50 Epifluorescence Microscope (Olympus, Tokyo, Japan).

Isolation of ribbon-like structures from *Pyramimonas parkeae*: Cells of *P. parkeae* were collected from 1.0 L of a seven-day culture by centrifugation at 4 °C, 1,000 $\times g$ for 10 min, resuspended in fresh EMS medium and re-centrifuged. The cells were resuspended in 15 ml of EMS medium and incubated at 4 °C for 1 h, and then the flagella were detached from the cells by intense agitation of the centrifuge tube at maximum speed of a vibratory mixer (Taitec, Tokyo, Japan) for 2 min. Deflagellated cells were collected by centrifugation at 4 °C, 100 $\times g$ for 10 min, and then resuspended in 10 ml EMS medium. Discharge of ribbon-like structures from the cells was induced by adding 100 μL of 4N HCl. Cells were pelleted by centrifugation at 4 °C, 100 $\times g$ for 10 min, and this process was repeated until the cells were completely removed. The supernatant, containing the ribbon-like structures, was centrifuged at 4 °C, 16,000 $\times g$ for 1.5 min to form a pellet of ribbons. The pellet of ribbons was washed several times by centrifugation at 4 °C, 16,000 $\times g$ for 1.5 min with EGTA medium (5 mM Tris-HCl, 5 mM EGTA, pH 7.5). The purified ejectosome ribbons were stored at -80 °C until use.

Tricine-sodium dodecyl sulfate-polyacrylamide gel electrophoresis: Purified ribbon-like structures were suspended in SDS sample buffer (50 mM Tris-HCl pH 6.8, 1% w/v SDS, 0.1% w/v dithiothreitol, 20% v/v glycerol) and incubated at room temperature for 30 min, followed by centrifugation at 4 °C, 16,000 $\times g$ for 15 min. Tricine-sodium dodecyl sulfate-polyacrylamide gel electrophoresis (Tricine-SDS-PAGE) was performed to separate small peptides below 10 kDa according to the method of Schägger and Jagow (1987). The gel was stained with 0.05% toluidine blue (Wako) in 25% methanol and 5% glycerol for 15 min at room temperature, and then de-stained with 25% methanol for 15 min. Protein bands were stained with 0.25% Coomassie brilliant blue R-250 in 30% methanol and 10% acetic acid during approximately 30 min, and background dye was de-stained in 30% methanol and 10% acetic acid for 3 h by renewing the de-staining solution several times.

Amino acids composition analysis: Approximately 100 μg of purified ribbon-like structures were hydrolyzed in 300 μl of 6N HCl for 24 hours at 110 °C, and 40 μl of digested aliquot was analyzed with an Amino Acid Analyzer L-8900 (Hitachi, Tokyo, Japan).

Monosaccharide composition analysis: Approximately 5 μg of purified ribbon-like structures were hydrolyzed in 300 μl of 4 M trifluoroacetic acid at 100 °C for 3 hours. The hydrolyzed sample was acetylated with acetic anhydride, and then fluorescence labeled monosaccharide was analyzed with BioAssist eZ (Toso, Tokyo, Japan).

Purification of proteins from the SDS-polyacrylamide gel: Each visualized band was excised from the SDS-polyacrylamide gel and incubated in distilled water at 4 °C for 12 h to elute proteins. Ten volumes of ice-cold acetone was added to the eluted aliquot and incubated at -25 °C for 1 h, followed by centrifugation at 4 °C, 16,000 $\times g$ for 30 min. The supernatant was carefully discarded and the pellet air-dried. The dried pellet was resuspended with 5% acetonitrile containing 0.1% trifluoroacetic acid, and purified with GL-Tip GC (GL Sciences, Tokyo, Japan), a sample preparation tip column packed with highly purified graphite designed for desalting and enriching particularly hydrophilic peptide samples, according to

manufacturer's instruction. Aliquots eluted from a column with 80% acetonitrile containing 0.1% trifluoroacetic acid were used for further Edman degradation.

Edman degradation: Protein aliquots (in 80% acetonitrile containing 0.1% trifluoroacetic acid) purified from the gel or electrophoretically transferred PVDF membrane were subjected to Edman degradation (APRO Science, Tokushima, Japan).

In-gel digestion: N-terminal blocked proteins were enzymatically digested into peptide fragments by an in-gel digestion method, and their N-terminal amino acids were sequenced. Each visualized protein band was excised from the tricine-SDS-polyacrylamide gel and de-stained by several 50% methanol washes. De-stained gel pieces were incubated in 50% acetonitrile for 10 min at room temperature, following dehydration with 100% acetonitrile for 10 min at room temperature. Dehydrated gel pieces were rehydrated with a digestion buffer (0.125 M Tris, 0.1% SDS, and 1 mM EDTA, pH 6.8) for 10 min at room temperature, and then again dehydrated with 100% acetonitrile for 10 min at room temperature. The dehydrated gel was again rehydrated with the digestion buffer, and then incubated in 50% acetonitrile (in the digestion buffer) for 10 min at room temperature, following two 10 min dehydrations in 100% acetonitrile at room temperature. Completely dehydrated gel pieces were air-dried for 1 h at room temperature, and treated with 6 μ l of Staphylococcus V8 protease solution (2 μ g/ μ l in the digestion buffer) overnight at 30 °C. Gel pieces containing digested peptide fragments were applied on a tricine-SDS-PAGE gel and electrophoretically resolved. The peptide bands separated in the SDS-PAGE were transferred onto PVDF membranes, and excised bands were subjected to Edman degradation.

Liquid chromatography-tandem mass spectrometry (LC/MS/MS): NanoLC/MS/MS analyses of samples digested by an in-gel digestion with trypsin were performed by Japan Proteomics Co., LTD (Sendai, Japan).

Western blotting: The tricine-SDS-PAGE of purified ribbon-like structures was performed as previously described, and separated proteins were electrophoretically transferred onto a PVDF membrane. The PVDF membrane was incubated with blocking reagent (TBST:20 mM Tris, 150 mM NaCl, 0.05% Tween 20, 1% w/v BSA) for 60 min at room temperature, and then incubated with rabbit histone H3 (ab1791: Abcam, Tokyo, Japan), H2A (GTX129418: Gene Tex, Irvine, CA, USA), H2B (GTX129434: Gene Tex) and H4 (GTX129560: Gene Tex) polyclonal antibodies diluted 1:2000 in TBST for 60 min at room temperature with gentle agitation. After three 5 min rinses with TBST, the membranes were incubated with alkaline-phosphatase-conjugated anti-rabbit IgG (Promega, Madison, WI, USA) diluted 1:5000 in TBST for 30 min at room temperature. After three 5 min rinses with TBST, immunoreactive bands were visualized with 5-bromo-4-chloro-3-indolyl phosphate and nitro blue tetrazolium (Promega).

Indirect immunofluorescence microscopy analysis: Purified ribbon-like structures were adhered to a poly-L-lysine (Sigma-Aldrich) coated cover glass, and incubated in PBS-BSA for 1 hour at 37 °C for blocking. After three 1 min rinses with PBS, samples were incubated for 1 hour at 37 °C with rabbit polyclonal antibody against histone H3 (1/1000 in PBS) (Abcam), histone H2A (1/1000 in PBS) (Gene Tex), histone H2B (1/1000 in PBS) (Gene Tex), histone H4 (1/1000 in PBS) (Gene Tex), and non-immunized rabbit serum (10% in PBS v/v) as negative control. After five 3 min rinses with PBS, samples were incubated with FITC-linked anti rabbit IgG for 1 hour at 37 °C. After five 3 min rinses with PBS, samples were mounted in 50% glycerol-PBS containing 0.1% *p*-phenylenediamine and observed with a BX-50 Epifluorescence Microscope (Olympus). For immunofluorescence analysis of the ribbons before

release from the cell, cells of *P. parkeae* were fixed for 15 min at room temperature with 3% formaldehyde (Wako Pure Chemical) in fixation buffer, given three 3 min rinses with PBS, and adhered to a poly-L-lysine (Sigma-Aldrich) coated cover glass. After three 1 min rinses with PBS, samples were incubated in PBS-BSA for 1 hour at 37 °C for blocking. After three 1 min rinses with PBS, samples were incubated for 1 hour at 37 °C with rabbit polyclonal antibody against histone H3 (1/1000 in PBS) (Abcam). After five 3 min rinses with PBS, samples were incubated with FITC-linked anti rabbit IgG for 1 hour at 37 °C. After five 3 min rinses with PBS, sample were mounted with 50% glycerol-PBS containing 0.1% *p*-phenylenediamine and observed with a BX-50 Epifluorescence Microscope (Olympus).

Enzyme treatments: Purified ribbon-like structures (approximately 10 μ g) were treated with 5 μ l of proteinase K solution (50 μ g/ml in DW containing 10 mM CaCl₂) (Wako Pure Chemical) for 6 hours at 50 °C or 5 μ l of lysozyme from hen white egg (10 mg / ml in PBS) (Seikagaku Biobusiness Corporation, Tokyo, Japan) for 24 hours at 37 °C. Treated samples (approximately 10 μ g) were suspended with 5 μ l of sample buffer (100 mM Tris-HCl at pH 6.8, 2% w/v SDS, 0.2% w/v dithiothreitol, 40% v/v glycerol) and applied to tricine-SDS-PAGE gels as described above. Gels were stained with toluidine blue and de-stained as described above. The de-stained gel was imaged, and then again de-stained until dye was completely removed in preparation for further Coomassie staining. The purified ribbon-like structures (approximately 10 μ g) also were treated with 5 μ l of DNase I solution (27 Kunitz units in RDD buffer that was supplied by the manufacture) (Qiagen, Hilden, Germany) or 5 μ l of RNase A solution (Qiagen) (50 μ g/ml in DNase-free water) for 24 hours at 37 °C, and treated samples were observed with optical microscopy.

Reconstruction assay in vitro using recombinant core histone proteins: Two μ l (in TBS) of the purified aliquot from the toluidine blue stained-bands (1.7 kDa to 4.6 kDa) and 10 μ l of recombinant human histone octamers that were collected and pooled by gel filtration purification of only fractions corresponding to the octamers (0.1 μ g; two each of histones H2A, H2B, H3 and H4) (accession numbers: H2A-POC0S8; H2B-P62807; H3-P68431; H4-P62805) (EpiCypher, NC, USA) were transferred to a 0.2 ml PCR tube, and were reacted at room temperature for 5 min. The reactants were adhered to a poly-L-lysine (Sigma-Aldrich, St. Louis, MO, USA) coated coverglass, and observed by indirect immunofluorescence microscopy using rabbit polyclonal antibody against histone H3 (1/1000 in PBS) (Abcam) and toluidine blue staining.

Extraction of total RNA: Approximately 100 mg of *P. parkeae* and *P. amylicifera* cells were collected by centrifugation at 4 °C, 1,000 \times *g* for 10 min, followed by washing once with fresh EMS medium and centrifugation at 4 °C, 1,000 \times *g* for 10 min. Approximately 50 μ g of total RNA was extracted with an RNeasy Plant Mini Kit (Qiagen), according to the manufacturer's instructions. Contaminating DNA was removed during RNA purification with an RNase-Free DNase Set (Qiagen), according to the manufacturer's instructions. The quality of extracted total RNA was assessed with a 2100 Bioanalyzer (Agilent Technologies, Santa Clara, CA, USA).

Transcript assembly and analysis: cDNA library preparation, sequencing of the library and transcript assembly were performed by BGI (Beijing, China). The cDNA library was prepared using TruSeq™ RNA Sample Prep Kit (Illumina, San Diego, CA, USA) according to manufacturer's instruction, and their quantifications and qualifications were checked using 2100 Bioanalyzer (Agilent Technologies) and StepOnePlus Real-Time PCR System (ABI, Foster, CA, USA). The libraries were sequenced using HiSeq™ 2000 (Illumina).

Transcriptome de novo assembly was performed with short reads assembling program, Trinity (release-20130225) (<http://trinityrnaseq.sourceforge.net/>) using the following parameters: `–seqType fq –min_contig_length 100; –min_glue 3 –group_pairs_distance 250; –ath_reinforcement_distance 85 –min_kmer_cov 3`. To capture sequences of core histones, all of unigenes assembled in *P. parkeae* and *P. amyliifera* were subjected to a BLAST search against the NCBI non-redundant protein database of core histones. We also performed additional analyses of conserved domains of the histone sequences using InterProScan (www.ebi.ac.uk/interpro/) or according to a definition by Sandman and Reeve (2006). DDBJ/EMBL/GenBank accessions for the raw data before the assembly: DRA003588. The unigenes are available on a web site (yama9803.html.xdomain.jp).

Phylogenetic analysis: In order to assume the phylogenetic positions of the core histone H3, H2A and H2B sequences identified from *Pyramimonas parkeae* and *Pyramimonas amyliifera* in this study, we performed preliminary molecular phylogenetic analyses with a broad taxon sampling, including major eukaryotic lineages such as Opisthokonta, Archaeplastida, Stramenopiles, Arveolata, Rizaria, Hacrobia, and Excavata. A multiple alignment of amino acid sequences for each histone H3, H2A, and H2B dataset was conducted using MUSCLE algorithm (Edgar 2004), implemented in MEGA6 (Tamura et al. 2013), and ambiguous sites were excluded from the datasets using a ‘gappyout’ command in trimAl (Capella-Gutiérrez et al. 2009). Molecular phylogenetic trees were constructed using the neighbor-joining method with JTT distances (Jones et al. 1992), implemented in MEGA6. Trees were rooted using a mid-point rooting.

Based on the results of the preliminary analysis, we performed additional phylogenetic analyses with a limited number of OTUs, including taxa from Glaucocystophyta, Rhodophyta, and Viridiplantae. As the same manner in the preliminary analysis, a multiple alignment of amino acid sequences for each Histone H3, H2A, and H2B dataset was conducted using MUSCLE algorithm, implemented in MEGA6, and ambiguous sites were excluded from the datasets using trimAl. As a result, 127, 145, and 136 amino acid positions were included in the final dataset of histone H3 (13 OTUs), H2A (15 OTUs) and H2B (15 OTUs), respectively. Molecular phylogenetic trees were constructed using the maximum likelihood (ML) and the Bayesian inference methods. A program Aminosan (Tanabe 2011) was used for choosing the best-fit amino acid substitution models via the corrected Akaike Information Criterion (Akaike 1974) for ML analysis, and the Bayesian Information Criterion (Schwarz 1978) for the Bayesian inference analysis.

The ML analysis was performed with 1,000 iterations of the likelihood-ratchet method (Vos 2003), implemented in Phylogear2-2.0.2013.10.22 (Tanabe 2013) and Treefinder (Jobb et al. 2004). Nodal support values were calculated using bootstrap method in ML, with 1,000 replicates for each dataset. Bayesian Inference analysis was performed with the selected model, using MrBayes5d-3.1.2.2012.12.13 (Tanabe 2012), a modified version of MrBayes 3.1 (Ronquist and Huelsenbeck 2003), for each dataset. The analysis was carried out by two simultaneous runs, each of which consisted of running four simultaneous chains for 1 million generations and sampling trees every 1,000 generations. Bayesian posterior probabilities were calculated after discarding the first 10% of the trees saved during MCMC as ‘burn-in’, based on results of the stationary states of log-likelihood analyzed using Tracer 1.6 (Rambaut et al. 2014). Glaucocystophyta and Rhodophyta were chosen as the outgroup taxa. DDBJ/EMBL/GenBank accessions for histone sequences of *P. parkeae* and *P. amyliifera* identified in this study: LC034583-LC034594.

Acknowledgements

We are grateful to Dr. Eric Henry for his valuable comments on the manuscript. This study was supported by a young scientific research grant from the Japan Society for Promotion of Sciences to T. Y. (Project Numbers: 25840128).

Appendix A. Supplementary data

Supplementary data associated with this article can be found, in the online version, at <http://dx.doi.org/10.1016/j.protis.2015.08.003>.

References

- Akaike H (1974) A new look at the statistical model identification. *IEEE Trans Autom Control* **19**:716–723
- Ammermann S, Hillebrand H, Rhiel E (2014) Further investigations on the polypeptides and reconstitution of prasinocyan ejectisomes. *Eur J Protistol* **50**:248–257
- Anderson TF, Preer JR, Preer LB, Bray M (1964) Studies in killing particles from *Paramecium*: the structure of refractile bodies from kappa particles. *J Microsc* **3**:395–402
- Capella-Gutiérrez S, Silla-Martínez JM, Gabaldón T (2009) trimAl: a tool for automated alignment trimming in large-scale phylogenetic analyses. *Bioinformatics* **25**:1972–1973
- Cavalier-Smith T (1982) The Evolutionary Origin and Phylogeny of Eukaryote Flagella. In Amos WB, Duckett JG (eds) *Prokaryotic and Eukaryotic Flagella*. Cambridge Univ. Press, London, pp 465–494
- Edgar RC (2004) MUSCLE: multiple sequence alignment with high accuracy and high throughput. *Nucleic Acids Res* **32**:1792–1797
- Eriksson S, Kim SK, Kubista M, Nordén B (1993) Binding of 4',6-diamidino-2-phenylindole (DAPI) to AT regions of DNA: Evidence for an allosteric conformational change. *Biochemistry* **32**:2987–2998
- Fusté MC, Simon-Pujol MD, Marques AM, Guinea J, Congregado F (1986) Isolation of a new free-living bacterium containing R-bodies. *J Gen Microbiol* **132**:2801–2805
- Gornik SG, Ford KL, Mulhern TD, Bacic A, McFadden GI, Waller RF (2012) Loss of nucleosomal DNA condensation coincides with appearance of a novel nuclear protein in dinoflagellates. *Curr Biol* **22**:2303–2312
- Hausmann K (1978) Extrusive organelles in protists. *Int Rev Cytol* **52**:197–279
- Heruth DP, Pond FR, Dilts JA, Quackenbush RL (1994) Characterization of genetic determination for R body synthesis and assembly in *Caedibacter taeniospiralis* 47 and 116. *J Bacteriol* **176**:3559–3569
- Hovasse R (1965) Trichocystes corps trichocystoides, cnidocystes et colloblastes. *Protozoologia* **3**:1–57

- Jeblick J, Kusch J** (2005) Sequence, transcription activity, and evolutionary origin of the R-body coding plasmid pKAP298 from the intracellular parasitic bacterium. *J Mol Evol* **60**:164–173
- Jobb G, von Haeseler A, Strimmer K** (2004) TREEFINDER: A powerful graphical analysis environment for molecular phylogenetics. *BMC Evol Biol* **4**:18
- Jones DT, Taylor WR, Thornton JM** (1992) The rapid generation of mutation data matrices from protein sequences. *Comput Appl Biosci* **8**:275–282
- Kasai K, Kawachi M, Erata M, Mori F, Yumoto K, Sato M, Ishimoto M** (2009) NIES-Collection, List of strains, 8th edition. *Jpn J Phycol* **57**:220
- Kopp S** (1976) Topographical distribution of sulphated glycosaminoglycans in human temporomandibular joint disks. *Oral Pathol Med* **5**:265–276
- Kugrens P, Lee RE, Corliss JO** (1994) Ultrastructure, biogenesis, and function of extrusive organelles in selected non-ciliate protist. *Protozoology* **181**:164–190
- Lalucat JO, Meyer O, Meyer F, Pares R, Schlegel HG** (1979) R bodies in newly isolated free-living hydrogen-oxidizing bacteria. *Arch Microbiol* **121**:9–15
- Maruyama S, Kim E** (2013) A modern descendant of early green algal phagotrophs. *Curr Biol* **23**:1081–1084
- Melasniemi H, Hernesmaa A** (2000) Yeast spores seem to be involved in biological phosphate removal: a microscopic in situ case study. *Microbiology* **146**:701–707
- Morrall S, Greenwood AD** (1980) A comparison of the periodic substructure of the trichocysts of the Cryptophyceae and Prasinophyceae. *BioSystems* **12**:71–83
- Okamoto N, Inouye I** (2005) The katablepharids are a distinct sister group of the Cryptophyta: a proposal for Katablepharidophyta division nova/Katablepharida phylum novum based on SSU rDNA and beta-tubulin phylogeny. *Protist* **156**:163–179
- Parke M, Adams I** (1965) Three species of Halosphaera. *J Mar Biol Ass UK* **45**:537–557
- Pearson BR, Norris RE** (1975) Fine structure of cell division in *Pyramimonas parkeae* Norris and Peason (Chlorophyta, Prasinophyceae). *J Phycol* **11**:113–124
- Pond FR, Gibson I, Lluat J, Quackenbush RL** (1989) R-body-producing bacteria. *Microbiol Rev* **53**:25–67
- Quackenbush RL** (1978) Genetic relationships among bacterial endosymbionts of *Paramecium aurelia*: deoxyribonucleotide sequence relationships among members of *Caedibacter*. *J Gen Microbiol* **108**:181–187
- Quackenbush RL** (1987) The Killer Trait. In Görtz HD (ed) *Current Topics in Paramecium research*. Springer, Berlin, pp 406–418
- Rambaut A, Suchard MA, Xie D, Drummond AJ** (2014) Tracer v1.6, Available from <http://beast.bio.ed.ac.uk/Tracer/>
- Rhiel E, Westermann M, Steiniger F, Kirchhoff C** (2013) Isolation and characterization of the ejectisomes of the prasinopyte *Pyramimonas grossii*. *Protozoology* **250**:1351–1361
- Ronquist F, Huelsenbeck JP** (2003) MrBayes 3: Bayesian phylogenetic inference under mixed models. *Bioinformatics* **19**:1572–1574
- Sandman K, Reeve JN** (2006) Archaeal histones and the origin of the histone fold. *Curr Opin Microbiol* **9**:520–525
- Schägger H, Jagow G** (1987) Tricine-sodium dodecyl sulfate-polyacrylamide gel electrophoresis for the separation of proteins in the range from 1 to 100 kDa. *Anal Biochem* **166**:368–376
- Schwarz G** (1978) Estimating the dimension of a model. *Ann Stat* **6**:461–464
- Scott JE, Dorling J** (1965) Differential staining of acid glycosaminoglycans (mucopolysaccharides) by alcian blue in salt solutions. *Histochemistry* **5**:221–233
- Tamura K, Stecher G, Peterson D, Filipski A, Kumar S** (2013) MEGA6: molecular evolutionary genetics analysis version 6. *O. Mol Biol Evol* **30**:2725–2729
- Tanabe AS** (2011) Kakusan4 and Aminosan: two programs for comparing nonpartitioned, proportional, and separate models for combined molecular phylogenetic analyses of multilocus sequence data. *Mol Ecol Resour* **11**:914–921
- Tanabe AS** (2012) MrBayes5d Version 3.1.2.2012.12.13, Available from URL: <http://www.fifthdimension.jp/>
- Tanabe AS** (2013) Phylogears Version 2.0.2013.10.22, Available from URL: <http://www.fifthdimension.jp/>
- Tijssen JPF, Beekes HW, Steveninck JV** (1982) Localization of polyphosphates in *Saccharomyces fragilis*, as revealed by 4',6-diamidino-2-phenylindole fluorescence. *Biochim Biophys Acta* **721**:394–398
- Volpi N, Maccari F** (2002) Detection of submicrogram quantities of glycosaminoglycans on agarose gels by sequential staining with toluidine blue and Stains-All. *Electrophoresis* **23**:4060–4066
- Vos RA** (2003) A accelerated likelihood surface exploration: the likelihood ratchet. *Syst Biol* **52**:368–373
- Wells B, Horne RW** (1983) The ultrastructure of *Pseudomonas avenae*. II. Intracellular refractile (R-body) structure. *Micron Microsc Acta* **14**:329–344
- Yabuki A, Kamikawa R, Ishikawa SA, Kolisko M, Kim E, Tanabe AS, Kume K, Ishida K, Inagaki Y** (2014) *Palpitomonas bilix* represents a basal cryptist lineage: insight into the character evolution in Cryptista. *Sci Rep*, <http://dx.doi.org/10.1038/srep04641>
- Yamagishi T, Kai A, Kawai H** (2012) Trichocyst ribbons of a cryptomonads are constituted of homologs of R-body proteins produced by the intracellular parasitic bacterium of *Paramecium*. *J Mol Evol* **74**:147–157